Supporting Information

Octahedral Pt_2CuNi Uniform Alloy Nanoparticle Catalyst with High Activity and Promising Stability for Oxygen Reduction Reaction

Changlin Zhang, William Sandorf, and Zhenmeng Peng*

Department of Chemical and Biomolecular Engineering
The University of Akron
Whitby Hall 211, Akron, OH 44325, United States
E-mail: zpeng@uakron.edu

Experimental

Materials

Platinum acetylacetonate ($Pt(acac)_2$, 97%) and nickel acetylacetonate ($Ni(acac)_2$, 95%) were purchased from Sigma-Aldrich. Acetone (C_3H_6O, 99.8%), chloroform ($CHCl_3$, 99.9%) and anhydrous ethanol (EtOH, 95.3%) were from Fisher Scientific. Concentrated perchloric acid ($HClO_4$, 70%) was from JT Baker. Carbon support (C, Vulcan® XC-72R) was purchased from Cabot. Commercial Pt/C (HP 20 wt.% Pt, Lot #591278) was purchased from fuel cell store. Hydrogen (H_2, 99.999%), carbon monoxide (CO, 99.999%), oxygen (O_2, 999.99%) and nitrogen (N_2, 99.999%) gases were obtained from Praxair.

Preparation of Octahedral Pt_2CuNi/C Uniform Alloy Nanoparticles

The octahedral Pt_2CuNi/C uniform alloy nanoparticles were prepared using a modified solid-state chemistry method,[1] which involved impregnation of both metal precursors on a C support and reducing them in CO and H_2 gas mixture. In a typical experiment for preparing the octahedral Pt_2CuNi/C (20 wt.% Pt), C was thermally treated in air at 300 ^oC overnight for removing moisture prior to use. $Pt(acac)_2$ (40 mg or 0.1 mmol), $Ni(acac)_2$ (13.1 mg or 0.05 mmol) and $Cu(acac)_2$ (13.3 mg or 0.05 mmol) were first dissolved in chloroform (4 mL), and then added drop wisely onto the pretreated C support (80 mg) under vigorous stirring. After the impregnation, the mixture was immediately transferred to a furnace which was then purged by N_2 flow for 20 minutes. The mixtures were reduced by being heated at a ramping rate of 15 °C/min to 200 °C and maintaining at the temperature for 1 hour in H_2/CO (5/120 cm^3/min). The gas atmosphere was switched back to N_2 and the product was cooled down to room temperature after the reaction is complete. The samples were then collected and stored in N_2 before any characterizations and testing.

The PtCu/C and octahedral PtNi/C samples were prepared using a similar procedure by adjusting the amounts of $Pt(acac)_2$ and $Ni(acac)_2$/$Cu(acac)_2$ precursors while keeping all other synthetic parameters the same.

Characterization

Transmission electron microscopy (TEM) images of the prepared samples were characterized with a JEOL JEM-1230 microscope operated at 120 KV. High-resolution TEM (HRTEM), high-angle annular dark field scanning TEM (HAADF-STEM), and energy dispersive X-ray (EDX) elemental maps and line scans of individual Pt_2CuNi/C nanoparticles were taken using a FEI Tecnai G2 F20 microscope operated at 200 KV. The X-ray diffraction (XRD) patterns were recorded on a Bruker AXS Dimension D8 X-Ray diffractometer with Cu Kα radiation source. Composition Analyses of the samples were performed using quantitative EDX equipped on a JEOL-7401 field emission scanning electron microscope (FESEM) with an operating voltage at 25 KV. The accurate metal loading in the products was determined by heating the samples at 10 °C/min to 750 °C in a flow of air (60 cm^3/min) and measuring weight of residue in a thermal gravimetric instrument (TA Instruments, Model Q50).

Rotating Disk Electrode (RDE) Catalyst Film Preparation

Thin catalyst films were drop-casted onto RDE for the electrochemical study. A glassy carbon electrode (5 mm in diameter) was polished using 0.05 μm alumina-particle suspension (Buehler) and rinsing with Millipore ultrapure DI water, which was followed by 2 min sonication and rinsing with DI water for three times. In a typical procedure for preparing the catalyst films, catalyst ink (1 mg catalyst/ml) was prepared by mixing sample powders with a stock solution containing DI water, iso-propanol, and Nafion ionomer (V_{water}: $V_{iso\text{-}propanol}$: $V_{5\%\ Nafion}$ = 0.6: 0.4: 0.004) and sonicating for 20 min. After that, 10 μL fresh ink was transferred onto the glassy

carbon electrode. The electrode was then mounted to a home-made electrode rotator and was rotated at a speed of 500 rpm and in a gentle air flow for around 15 min, which allowed the formation of uniform thin catalyst films.[2] For XRD characterization of reacted catalysts, catalyst powders were loaded onto a conductive carbon cloth by spaying and drying the ink on the surface, and tested under the same experimental conditions.

Electrochemical Measurements

The electrochemical experiments were conducted using a CHI 760D electrochemical workstation (CH Instruments, Inc.) and a rotating disk electrode controller (AFMSRCE, Pine Instrument Co.). A three-electrode system, consisting of the catalyst film-coated glassy carbon working electrode, a platinum wire counter electrode, and a HydroFlex reference electrode (ET070, Edaq Inc.), were used for all electrochemical measurements. The reference electrode was placed in one separate beaker and was connected to the reaction cell with a bridge tube. The reaction cell, the bridge tube and the beaker were filled using the same electrolyte. Prior to electrochemical measurement, glassware including the beaker, reaction cell, gas bubbler and bridge tube were soaked in boiling water for 4 hours and then rinsed with ultrapure water and dried in N_2. Solution resistance of the testing system was determined by electrochemical impedance spectroscopy (EIS). The potentials of the reference electrode were calibrated using a home-built reversible hydrogen electrode (RHE). All the potentials were recorded with respect to the HydroFlex electrode and were reported with respect to RHE in the discussion part.

The measurement of electrochemical active surface area (ECSA) of the catalysts was conducted in an N_2-protected 0.1 M $HClO_4$ aqueous solution at room temperature. The catalysts were first activated by sweeping in the potential range of 0.05 -1.00 V vs. RHE at a scan rate of 100 mV/s for 25 cycles to yield stable CV curves, which was followed by a few more CV cycles

using the same potential and scan parameters.[3] The ECSA values of the catalysts were calculated by integrating the area in hydrogen adsorption range (~0.05 - 0.40 V vs. RHE) from the backward sweep in the CV curves.

The oxygen reduction reaction (ORR) property of the Pt_2CuNi/C was studied using linear sweep voltammetry (LSV). The potential was swept from 0.2 V to 1.0 V at a scan rate of 10 mV/s and an electrode rotation rate of 1600 rpm in O_2-saturated 0.1 M $HClO_4$ aqueous solution. The kinetic currents (I_k) were calculated using the Koutecky-Levich equation:[4]

$$\frac{1}{I} = \frac{1}{I_k} + \frac{1}{B\omega^{1/2}} \quad (1)$$

where I is the measured current, B is constant and ω is the angular rotating frequency of the working electrode ($\omega = 2\pi f/60$, f is the RDE rotation rate in r.p.m.). The Ohmic iR drop during the ORR experiments was corrected for accurate measurement of the intrinsic ORR property.[5]

The catalyst stability was studied using an accelerated stability test, in which repetitive CV scans were performed between 0.60 and 1.00 V vs. RHE at a scan rate of 50 mV/s for 4,000 cycles (or 10,000 cycles) in 0.1 M $HClO_4$. After designated cycle scans, another 300 cycles of CV scan at 10 V/s between 0 and 1.00 V vs. RHE were first applied for cleaning the catalysts surface before any ECSA and ORR activity measurements.[6]

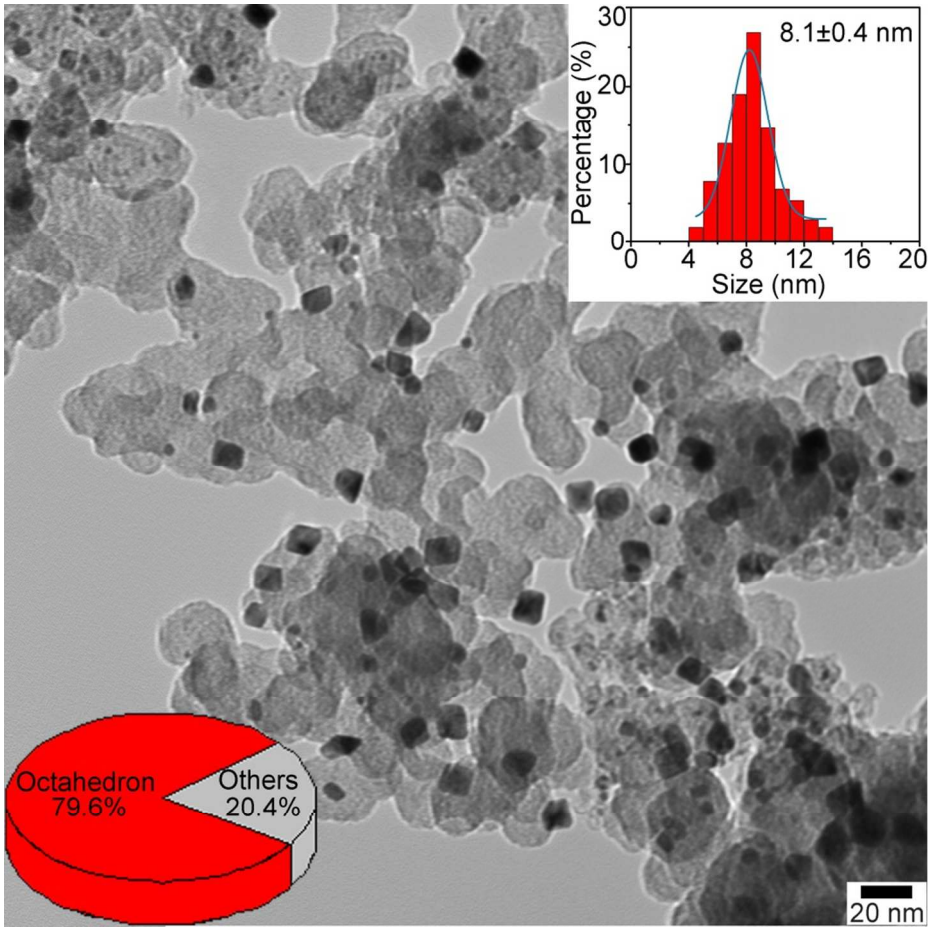

Figure S1. TEM image, size distribution, and yield analysis of as-prepared octahedral Pt_2CuNi/C nanoparticles.

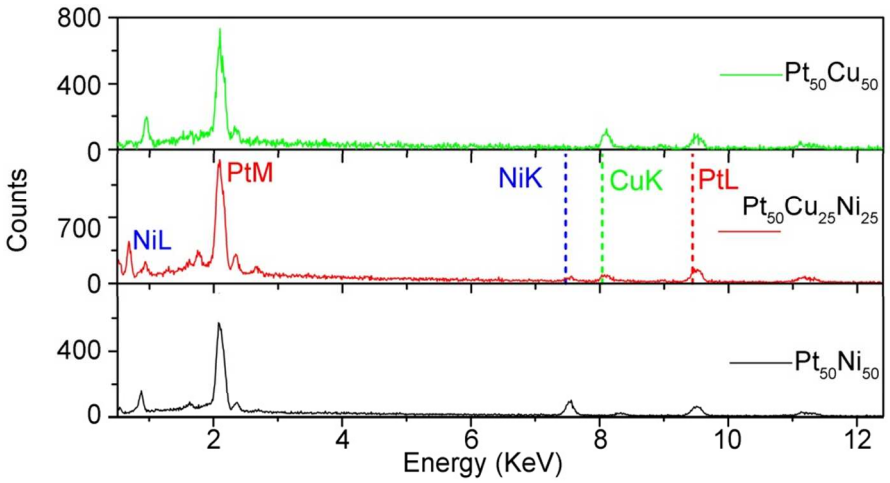

Figure S2. EDX spectra of as-prepared octahedral Pt_2CuNi/C, octahedral PtNi/C, and PtCu/C nanoparticles.

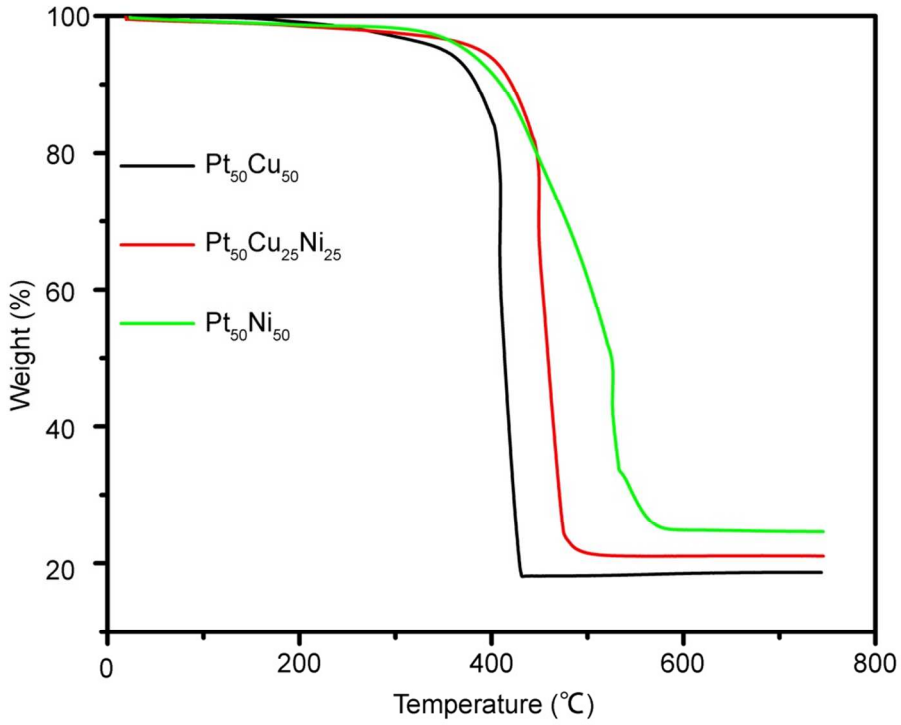

Figure S3. TGA curves of as-prepared octahedral Pt_2CuNi/C, octahedral PtNi/C, and PtCu/C nanoparticles.

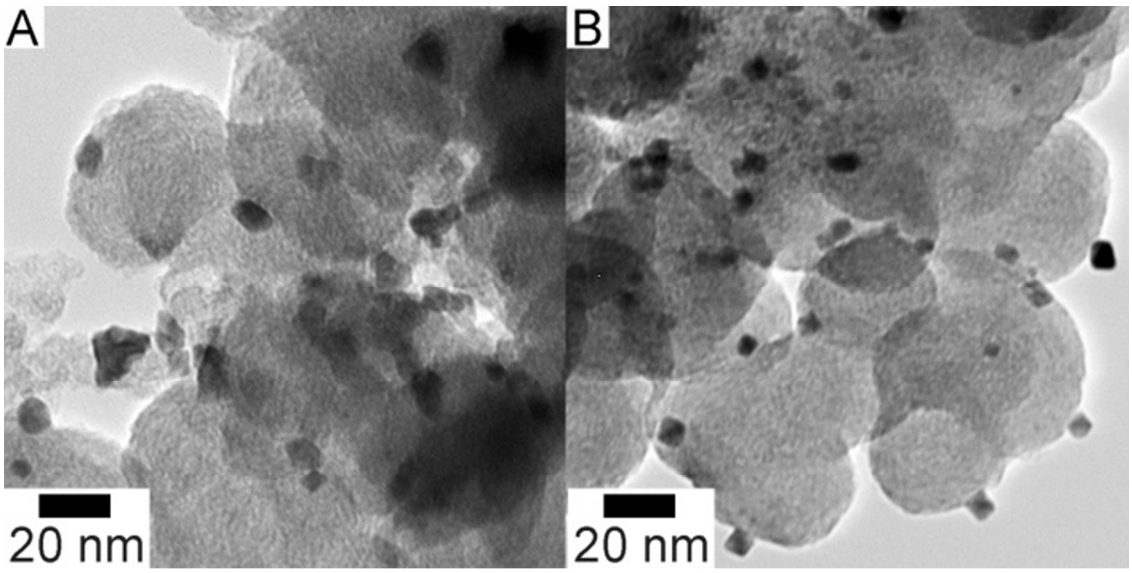

Figure S4. TEM images of as-prepared (A) PtCu/C and (B) octahedral PtNi/C nanoparticles.

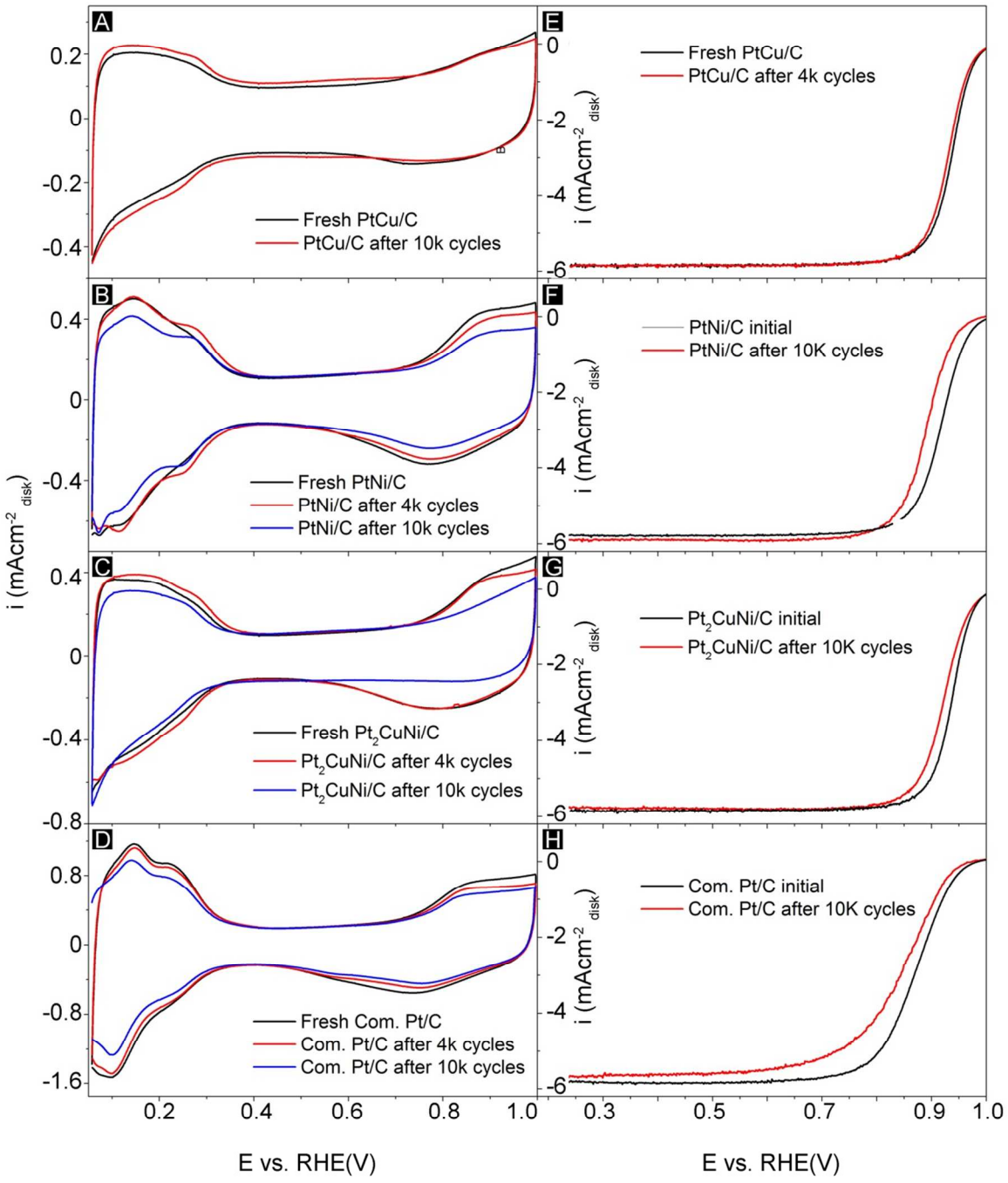

Figure S5. CVs and ORR polarization curves using the octahedral Pt_2CuNi/C, octahedral PtNi/C, PtCu/C, and commercial Pt/C catalysts before and after the stability test.

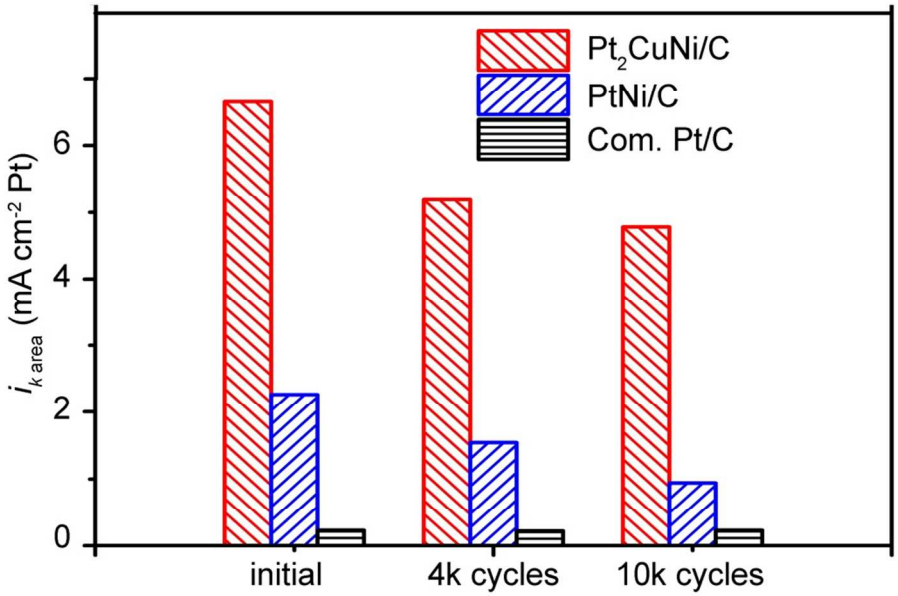

Figure S6. Area-specified activity of octahedral Pt_2CuNi/C, octahedral PtNi/C, and commercial Pt/C at 0.9 V vs. RHE before and after the stability test.

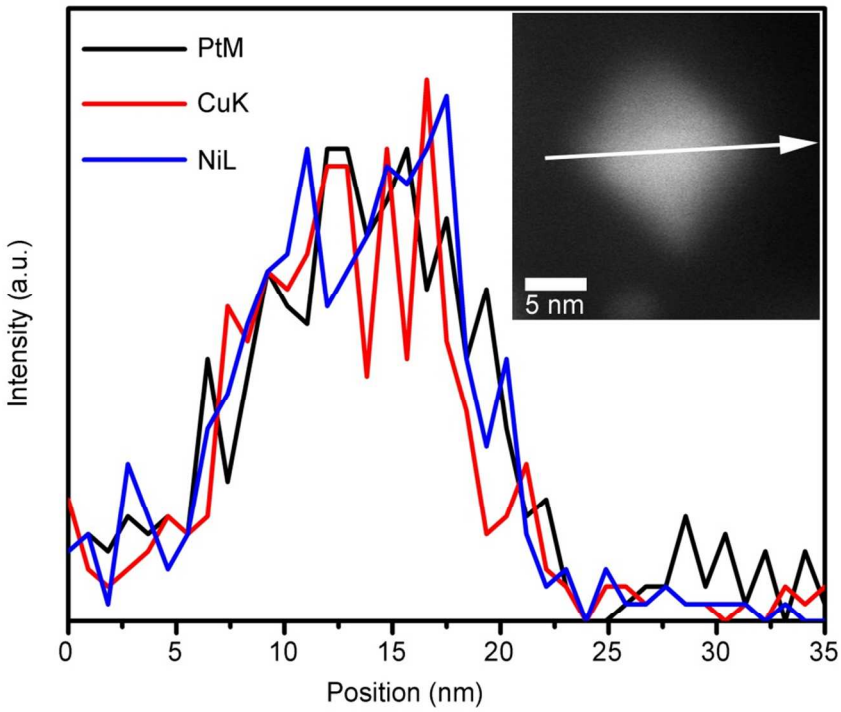

Figure S7. HAADF-STEM and EDX elemental line scans of the fresh Pt_2CuNi/C.

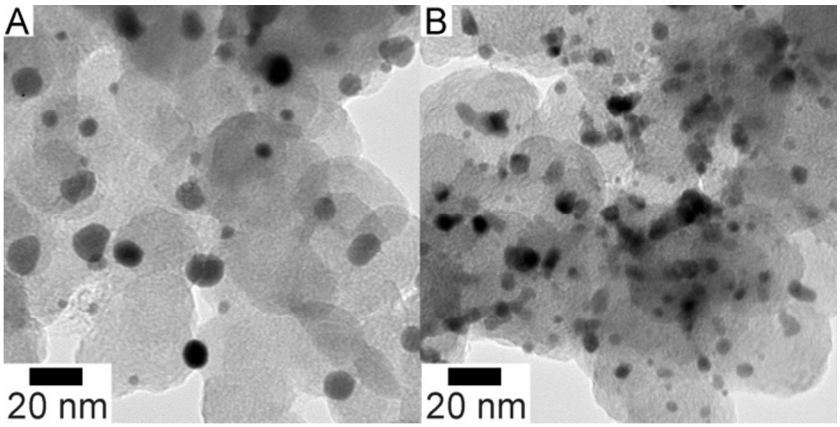

Figure S8. TEM images of (A) PtCu/C and (B) PtNi/C catalysts after 4,000 cycles of stability test.

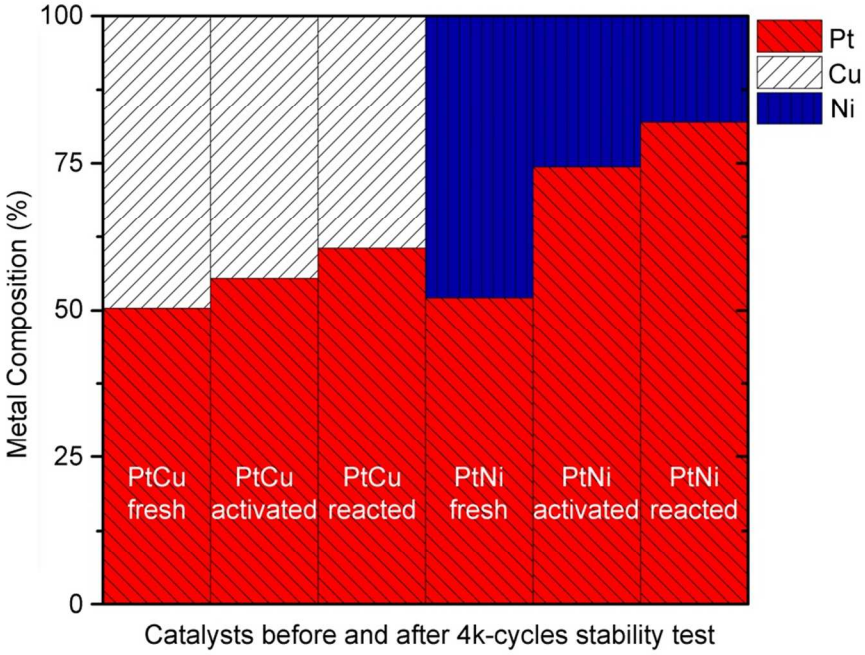

Figure S9. Particle composition of the octahedral PtNi/C, and PtCu/C before and after stability test.

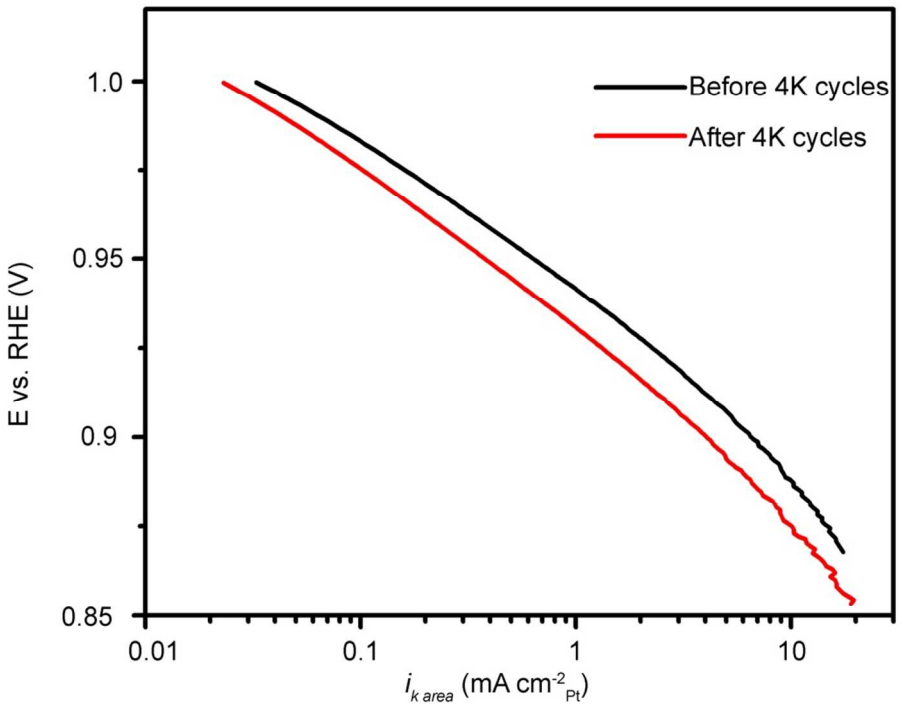

Figure S10. Tafel plots of the octahedral Pt_2CuNi/C before and after stability test.

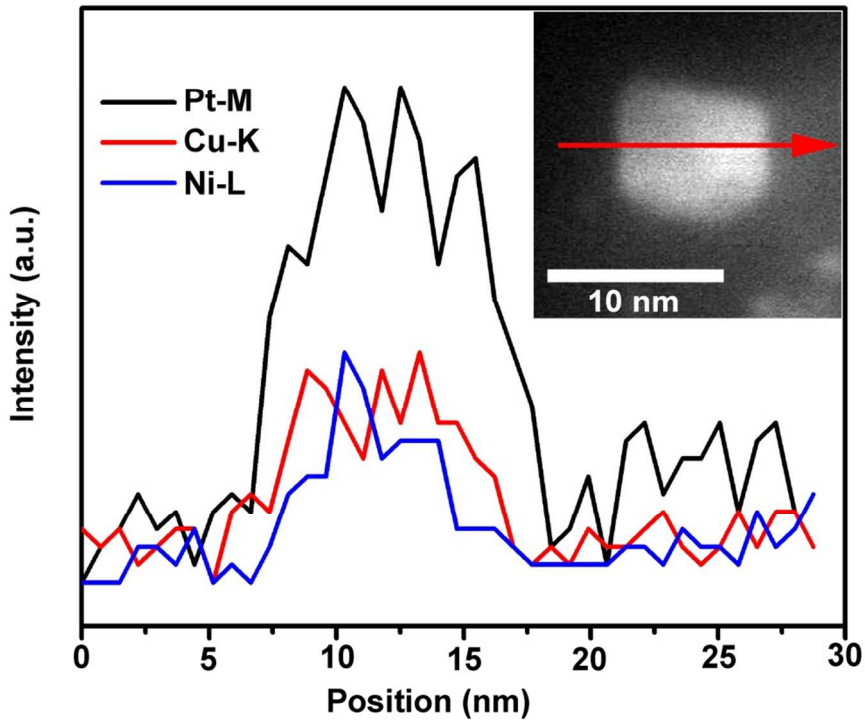

Figure S11. HAADF-STEM and EDX elemental line scans of reacted Pt_2CuNi/C.

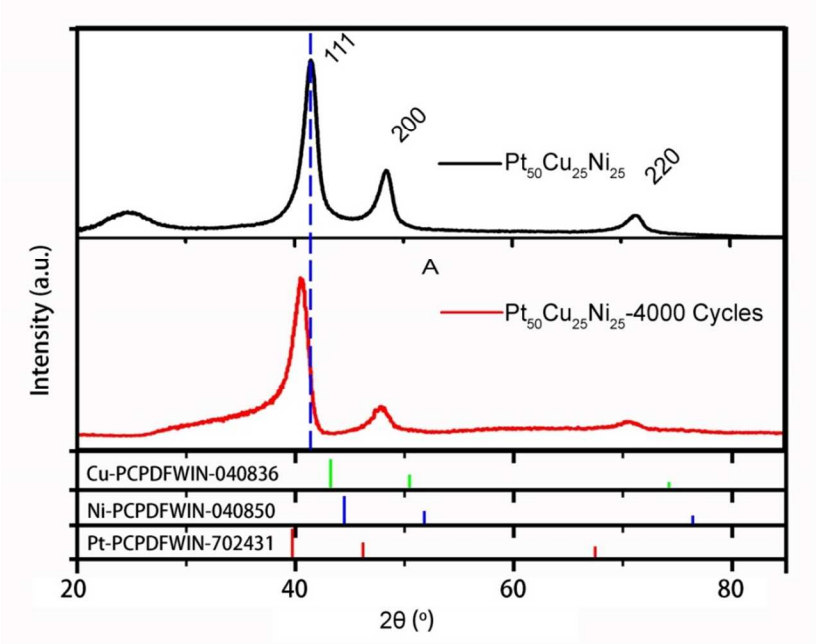

Figure S12. XRD patterns of fresh and reacted Pt_2CuNi/C, reference peak information for pure metal Pt, Cu and Ni being included for comparison.

Table S1. Comparison of ORR property of Pt-based alloy catalysts

Numer	Catalyst	MA@0.9V (A/mg Pt)	SA@0.9V (mA/cm² Pt)	Stability	Ref.
1	$PtCo_3$	0.34	0.49	NA	[7]
2	$PtCu_3Co$	0.37	0.34	NA	[7]
3	$PtCuCo_3$	0.49	0.44	NA	[7]
4	Pt_3Co-Acid Treated	0.35	0.74	NA	[8]
5	Pt_3Co-Annealing	0.52	1.10	10 mv shift in $E_{1/2}$	[4]
6	$Pt_{2.6}Ni$	1.6	NA	NA	[9]
7	$Pt_{2.5}Ni$	3.3	NA	40%	[9]
8	PtPd	NA	0.307	9 mv shift in $E_{1/2}$	[10]
9	PtNi	0.68	3.0	40%	[11]
10	$PtNi_{1.5}$	1.2	2.3	45%	[3]
11	PtNi	1.7	3.7	66%	[3]
12	$Pt_{1.5}Ni$	1.0	3.4	16%	[3]
13	PtCu/CuNW	1.24	2.65	36%	[12]
14	$Pt_{80}Fe_{20}$	0.84	1.53	<10%	[13]
15	$Pt_{92}Co_8$	NA	0.64	NA	[13]
16	Pt_2CuNi	2.35	6.65	<32%	This paper

REFERENCES

(1) Zhang, C.; Hwang, S. Y.; Trout, A.; Peng, Z. *J. Am. Chem. Soc.* **2014,** *136*, 7805-7808.
(2) Garsany, Y.; Singer, I. L.; Swider-Lyons, K. E. *J. Electroanal. Chem.* **2011,** *662*, 396-406.
(3) Cui, C.; Gan, L.; Heggen, M.; Rudi, S.; Strasser, P. *Nat. Mater.* **2013,** *12*, 765-771.
(4) Wang, D.; Xin, H. L.; Hovden, R.; Wang, H.; Yu, Y.; Muller, D. A.; DiSalvo, F. J.; Abruña, H. D. *Nat. Mater.* **2013,** *12*, 81-87.
(5) Vliet, D. v. d.; Strmcnik, D. S.; Wang, C.; Stamenkovic, V. R.; Markovic, N. M.; Koper, M. T. M. *J. Electroanal. Chem.* **2010,** *647*, 29-34.
(6) Holewinski, A.; Idrobo, J.-C.; Linic, S. *Nat. Chem.* **2014,** *6*, 828-834.
(7) Srivastava, R.; Mani, P.; Hahn, N.; Strasser, P. *Angew. Chem. Int. Ed.* **2007,** *46*, 8988-8991.
(8) Chen, S.; Ferreira, P. J.; Sheng, W.; Yabuuchi, N.; Allard, L. F.; Shao-Horn, Y. *J. Am. Chem. Soc.* **2008,** *130*, 13818-13819.
(9) Choi, S.-I.; Xie, S.; Shao, M.; Odell, J. H.; Lu, N.; Peng, H.-C.; Protsailo, L.; Guerrero, S.; Park, J.; Xia, X.; Wang, J.; Kim, M. J.; Xia, Y. *Nano Lett.* **2013,** *13*, 3420-3425.
(10) Peng, Z.; Yang, H. *J. Am. Chem. Soc.* **2009,** *131*, 7542-7543.
(11) Carpenter, M. K.; Moylan, T. E.; Kukreja, R. S.; Atwan, M. H.; Tessema, M. M. *J. Am. Chem. Soc.* **2012,** *134*, 8535-8542.
(12) Wittkopf, J. A.; Zheng, J.; Yan, Y. *ACS Catal.* **2014,** *4*, 3145-3151.
(13) Guo, S.; Li, D.; Zhu, H.; Zhang, S.; Markovic, N. M.; Stamenkovic, V. R.; Sun, S. *Angew. Chem. Int. Ed.* **2013,** *52*, 3465-3468.